

Cryogenic mechanical design of the Gemini South Adaptive Optics Imager (GSAOI)

Dejan Stevanovic* and John Hart

Research School of Astronomy and Astrophysics, The Australian National University
Cotter Road, Weston ACT 2611, Canberra, Australia

ABSTRACT

The Research School of Astronomy and Astrophysics (RSAA) of the Australian National University (ANU) has designed and constructed The Gemini South Adaptive Optics Imager (GSAOI) that will be used with the Multi-Conjugate Adaptive Optics system on the Gemini South telescope in Chile. GSAOI contains three cryogenic mechanisms; two filter wheels and a utility wheel. An approach to the athermalization of cryogenic mechanisms is presented. The 280 mm diameter filter wheels are athermalized using bi-material conical bearing seats where the bearing preload is constant, irrespective of temperature. The lens mounting method is also described. Lenses up to 170 mm in diameter are mounted within precision cells such that radial clearances reduce to zero at operating temperature. The method used to derive the room-temperature lens and cell dimensions is described. Lenses are preloaded axially against conical seats using wave washers. This technique has been used successfully to mount lenses of ~100 mm diameter in the Gemini Near-infrared Integral Field Spectrograph (NIFS), also designed and constructed by RSAA.

Keywords: mechanisms, cryogenic, optical mounts, GSAOI, Gemini

1. INTRODUCTION

In September 2001, RSAA proposed to perform a Conceptual Design Study for the Gemini South Adaptive Optics Imager (GSAOI). The RSAA was one of two groups selected to perform a CoD for the GSAOI. The Conceptual Design Study contract was signed with RSAA in April 2002. The Conceptual Design Review was held in August 2002. Based on this, RSAA was selected to perform the detailed design and construction of the instrument in December 2002. The Critical Design Review¹ was successfully conducted in October 2003 and the instrument is now in the construction and assembly phase.

The GSAOI² is a diffraction-limited near-infrared camera that will serve as the main science instrument to be used with the Multi-Conjugate Adaptive Optics (MCAO) system on the Gemini South telescope. GSAOI is required at Gemini South in early 2006 for MCAO commissioning. GSAOI contains a simple, yet high performance, re-imaging optical system. Two filter wheels accommodate an extensive range of near-infrared broad-band and narrow-band filters. A single utility wheel allows for the insertion of lenses to view the pupil image for alignment purposes, or defocused images for wave front quantification.

At the heart of the GSAOI is a state-of-the-art detector mosaic comprising four 2048×2048 pixel Rockwell HAWAII-2RG detectors, which form a 4096×4096 pixel mosaic. The Detector Control System (DCS) is based on the well known SDSU controller, so as to facilitate early instrument delivery. GSAOI will deliver excellent image quality with high throughput and high stability on a time scale commensurate with MCAO commissioning. These attributes will ensure that the Gemini community gains the maximum scientific return from its investment in MCAO and GSAOI.

* dejan@mso.anu.edu.au; Phone: +61 2 6125 0213, FAX: +61 2 6125 0233

This paper will address some of the mechanical design issues that were encountered during the GSAOI design phase. More specifically, the paper will address problems of lens mounting and mechanism implementation in a cryo-vacuum environment.

2. LENS MOUNTING SYSTEM

The most common problem that engineers encounter in designing for a cryogenic environment is the differential contraction at bimaterial interfaces. This is especially emphasized when a precision fit must be achieved. Commonly, this problem occurs in the process of mounting glass lenses in aluminium lens mounts. In addition, an adjustable lens mount assembly is often a requisite. Such an assembly must have high reliability and repeatability of the lens position, maintained within usually tight positional tolerances imposed on the optical elements in the cryogenic instruments.

2.1 General Concepts

There are two main issues to be considered when positioning a lens in a cryogenic environment: its axial position in the optical system and its radial (in-plane) position within the lens cell. The mounting concept that was applied to all GSAOI lenses is depicted in Fig. 1.

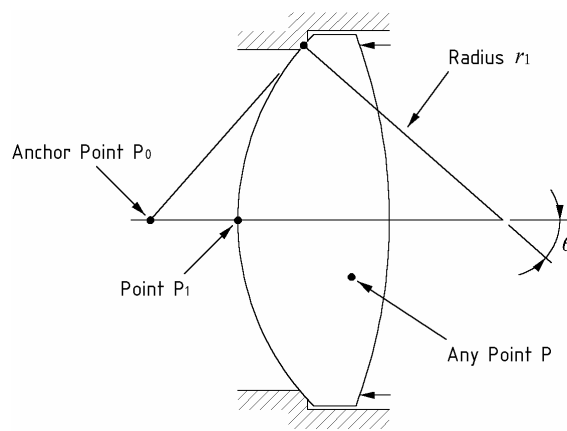


Fig. 1. Positional compensation geometry for lenses.

Radially, lenses in GSAOI are centered in close fitting aluminium bores. Radial tolerance compensation is obviously needed to allow for the differential contraction of the aluminium cell to the glass material of the lens. Determining this compensation correctly is of the major importance in order to protect lenses from being crushed in the cells during the cool-down process. Since all materials used are isotropic, the thermal strain is also isotropic and a simple scale factor can be applied to provide compensation. Axially, the lens is correctly positioned by being supported through the tangent conical surface of a front retainer, while being spring loaded from the back. The anchor point, P_0 , is the apex of the cone that is tangent to the lens at the circle where it contacts the retainer. As temperature changes, this is the point where there is to be no relative movement between the lens and mount. The relative displacement between the lens and mount at any point, P , is the product of the distance $P_0 - P$ and the thermal strain difference $\epsilon_{lens} - \epsilon_{mount}$. At the vertex of the mounted lens surface, point P_1 , this displacement is given by:

$$e_1 = r_1 \left(\frac{1 - \cos \theta}{\cos \theta} \right) (\epsilon_{lens} - \epsilon_{mount}) \quad (1)$$

where r_1 and θ are defined in Fig. 1.

This principle is applied to the cryogenic (cold) geometry to derive the ambient (warm) geometry. In this way the cold optical layout can be easily transferred to the warm layout by applying the thermal expansion factor of aluminium

between the anchor points for each of the lens cells (i.e. lens groups). The warm layout is then used to manufacture mounts and lenses. All lenses used in the GSAOI optical system were mounted in this fashion.

2.2 Application

The best representation for this mounting method is the GSAOI field lens doublet assembly, this being the biggest optical elements in the system. The GSAOI doublet field lens mount is depicted in Fig. 2. The mount has to retain the INFRASIL/CaF₂ doublet lenses, which are 170 mm in diameter and of a total mass of 2.35 kg. The mount is fixed from three sides in order to support the mass of the lenses with minimal deflection.

The first lens is fixed by a tangent contact retainer from the front side while the second lens is supported from the back side against the tangent retaining surface of the cell. A wave washer, positioned in between the lenses, spring loads both of them to accommodate any axial shrinkage of the lenses during cooling. At the same time, the lenses have sufficient radial clearance in the mount at ambient temperature to accommodate for zero theoretical radial clearance at the operating temperature of 70°K.

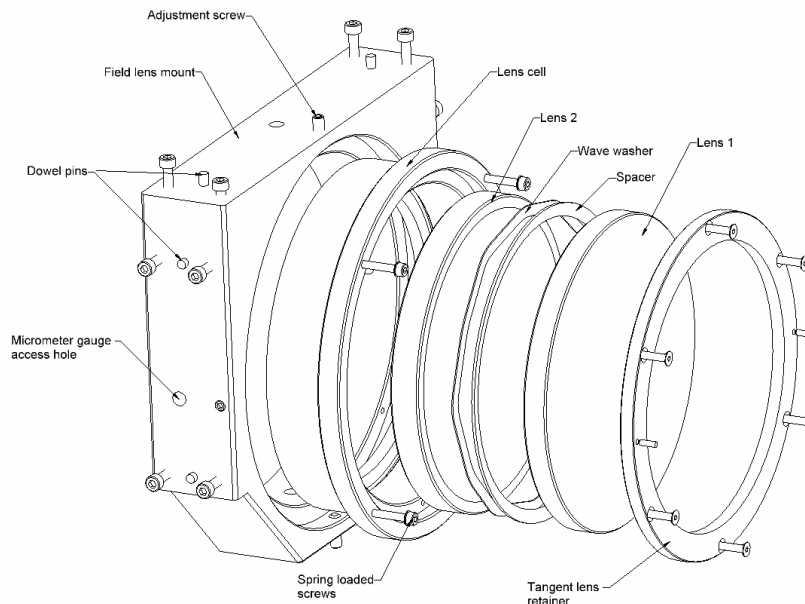


Fig. 2. Exploded view of the field lens mount.

The cell mount is dowel-registered within the optable, which served as the reference mechanical element for the whole optical system. The lenses are fixed in the cell, as explained above, but the lens cell is in-plane adjustable. This is achieved by using four adjustment set-screws in the mount. Holes are also provided in the mount for the micrometer gauges used during the alignment process to accommodate the correct positioning of the cell with repeatability of sufficient accuracy.

2.3 Lens Mount Safety

For all lens groups used in the GSAOI optical system, the thermal contraction of the aluminium alloy housing is greater than that of the lens at the operating temperature. The housing and lens tolerances are arranged such that the minimum theoretical lens/cell clearance is zero at this temperature.

During the cooling process the lens temperature will lag the housing temperature. It is therefore possible that a transient interference condition can develop, and potentially this can cause lenses damage. Hence, it is investigated here to ensure that this situation is avoided. If need be, the lens clearance can be increased at the cost of some increase in misalignment and consequent aberration.

The analysis used for GSAOI is conservative. With the cooling rate of the cryostat known, the temperature lag of the lenses is determined based on the assumption that they are cooled by radiation alone. The clearances between lenses and housings are then determined from these temperatures using the thermal strain relationships presented elsewhere³⁻⁶. The cryostat used for GSAOI is a replica of that produced for another Gemini instrument, namely the Near Infrared Imager (NIRI). Data obtained from the NIRI web site⁷ has been used to model the cooling rate of the cryostat.

If the time since the start of cooling is t (sec), then the temperature (K) of the cryostat cold work surface plate (and lens housings) is given by:

$$T_1 = 293 - 6.5237 \times 10^{-4} t + 2.7429 \times 10^{-10} t^2 + 2.8993 \times 10^{-16} t^3 \quad (2)$$

This relationship is plotted in Fig. 3.

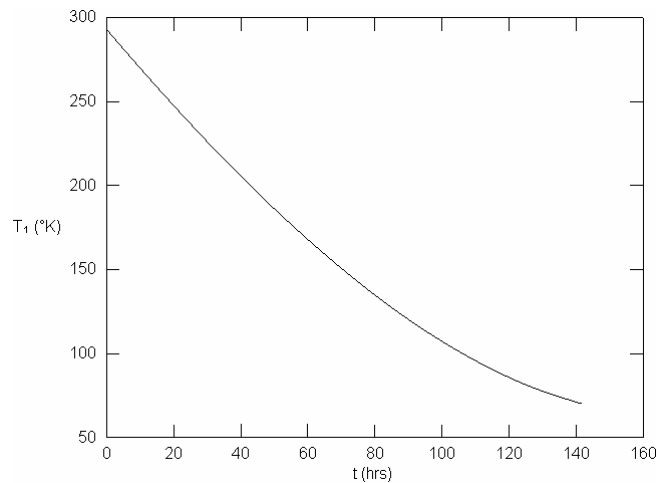


Fig. 3. Cryostat cooling curve.

The corresponding cryostat cooling rate is

$$\frac{dT_1}{dt} = -6.5237 \times 10^{-4} + 5.4858 \times 10^{-10} t + 8.6979 \times 10^{-16} t^2 \quad (3)$$

The lag in the lens temperature is dependent on the spatial character of the cavity containing it. If this volume is large compared to the lens, it behaves as a black body and the rate of heat transfer is independent of its emissivity (but not that of the lens). If the cavity is closely conforming to the lens, then both emissivities are involved, but if they are equal (as they will tend to be), the rate of heat transfer will be twice that applicable for a large cavity. Here, the cavity is assumed to be large because this is both near-realistic and conservative. The emissivity of the lenses is assumed to be unity because they transmit only over relatively narrow wavelength pass bands. Over the wide range of thermal wavelengths they will be largely absorptive. Where lenses are mounted as pairs, cooling will be slowed because they shield each other and the adjacent surfaces are effectively disabled as radiators. The temperature lag is also dependent on the specific heat capacity of the lens materials. In general it is known that this decreases considerably as temperature reduces. However, ambient-temperature values are used here because low-temperature data are not readily available. This assumption also makes the analysis conservative.

If the lens mass is m_2 , the lens specific heat capacity is C_2 , the lens radiating surface area is A_2 , the lens emissivity is ζ_2 , and the Stefan-Boltzmann constant is σ ($5.67051 \times 10^{-14} \text{ W mm}^{-2} \text{ K}^{-4}$), the lens temperature is expressed as:

$$T_2 = \left(T_1^4 - \frac{C_2 m_2}{\sigma A_2 \xi_2} \frac{dT_1}{dt} \right)^{\frac{1}{4}} \quad (4)$$

More correctly, the term dT_1/dt in this relationship should be dT_2/dt , but this simplifying assumption is justified because the difference is small.

The results of this analysis are presented for the worst lagging lens in the system, this being the calcium fluoride element of the field lens. The lens properties are shown in Table 1.

Table 1 Properties of the worst lagging lens

Identification	Material	C_2 ($\text{J kg}^{-1}\text{K}^{-1}$)	m_2 (kg)	A_2 (mm^2)	ξ_2
Field Lens 1	Calcium Fluoride	854	1.56	22700	1

The calculated temperature lag is plotted in Fig. 4.

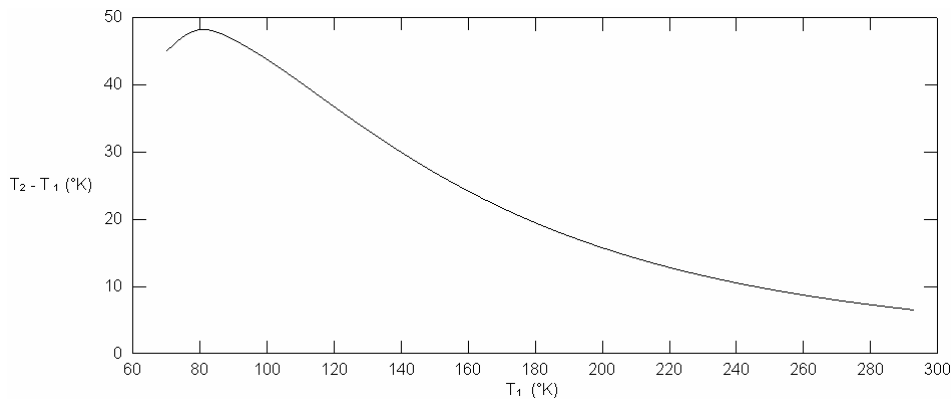


Fig. 4. Lens temperature lag during cryostat cooling.

The resulting ratio of lens diametral clearance to lens diameter is shown in Fig. 5.

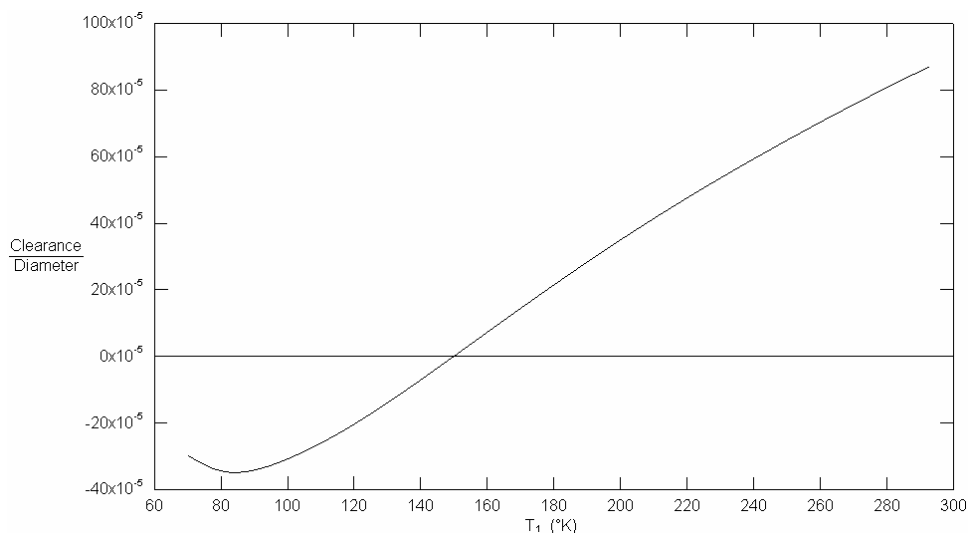


Fig. 5. Lens clearance to diameter ratio during cryostat cooling.

Slight interference develops at low temperature for this lens, and so a compensating increase in clearance is required. The diameter of the lens is 170 mm. The required clearance increase is 58 μm . This is smaller than the 65 μm width of the tolerance zone, and so has no significant effect on optical performance.

3. FILTER WHEEL MECHANISM

As shown in Fig. 6, two 15-position, 280mm in diameter, filter wheels, are to be located ahead of the system cold stop. These wheels will contain a range of broad-band and narrow-band imaging filters and a blocked position for measuring bias frames. Each filter is 42 mm in diameter with a working aperture of 32 mm and 28 mm, for the first and the second wheel filters, respectively. The total number of filters can be increased to a maximum of 27. This limit is set by space restrictions within the duplicate NIRI/NIFS cryostat. The issue of ensuring that two wheels are never simultaneously positioned at their clear positions has been implemented in the control software.

The filter wheels will be driven at their circumferences using spur gears with a two-stage reduction of 70:1. Each filter wheel will be driven independently using separate cryogenic stepper motors. At a stepper motor speed of 200 rpm, they will complete one revolution in 21 s, with a position repeatability of 0.05 mm. This performance meets the Gemini requirements of 30 s and 0.1 mm, respectively. The position repeatability of the filter wheels will meet requirements for flat field reproducibility where it is important that filters return accurately to their set positions.

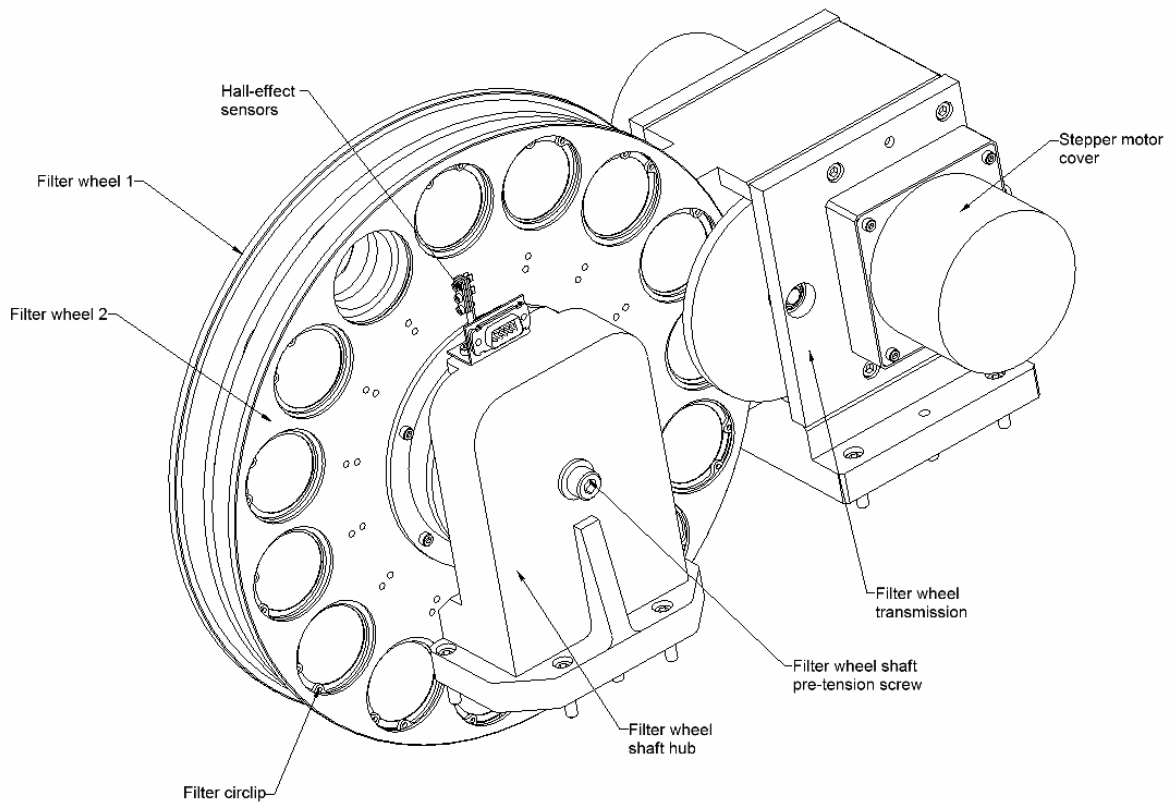


Fig. 6. Dual filter wheel mechanism – general layout.

The transmission and slipping-clutch system are illustrated in Fig. 7. The gear train is pushed against tapered-shaft seats by Belleville washers. In the normal operating condition, the friction force generated by this gear-shaft connection is sufficient to transfer the constant drive torque from the stepper motor. In the case of malfunction or wheel jam, the drive torque will increase rapidly, causing slippage between the gears and shafts without any damage to the gear train system. This protects the fine-pitch gearing (gear teeth module of 0.5) from damage.

The wheels will be position-stabilized by using friction disk brakes, depicted in Fig. 8. The friction brake will produce a force of 44 N at a radius of 35 mm, resulting in a constant drag torque of 308 Nmm. This will be more than sufficient to suppress any backlash in the gear train system and to achieve both, the required wheel stability of $< \pm 0.1$ mm (at the GSAOI detector), and the required tilt stability of $< \pm 0.4$ degrees. Individual filter positions will be encoded by Hall-effect sensors.

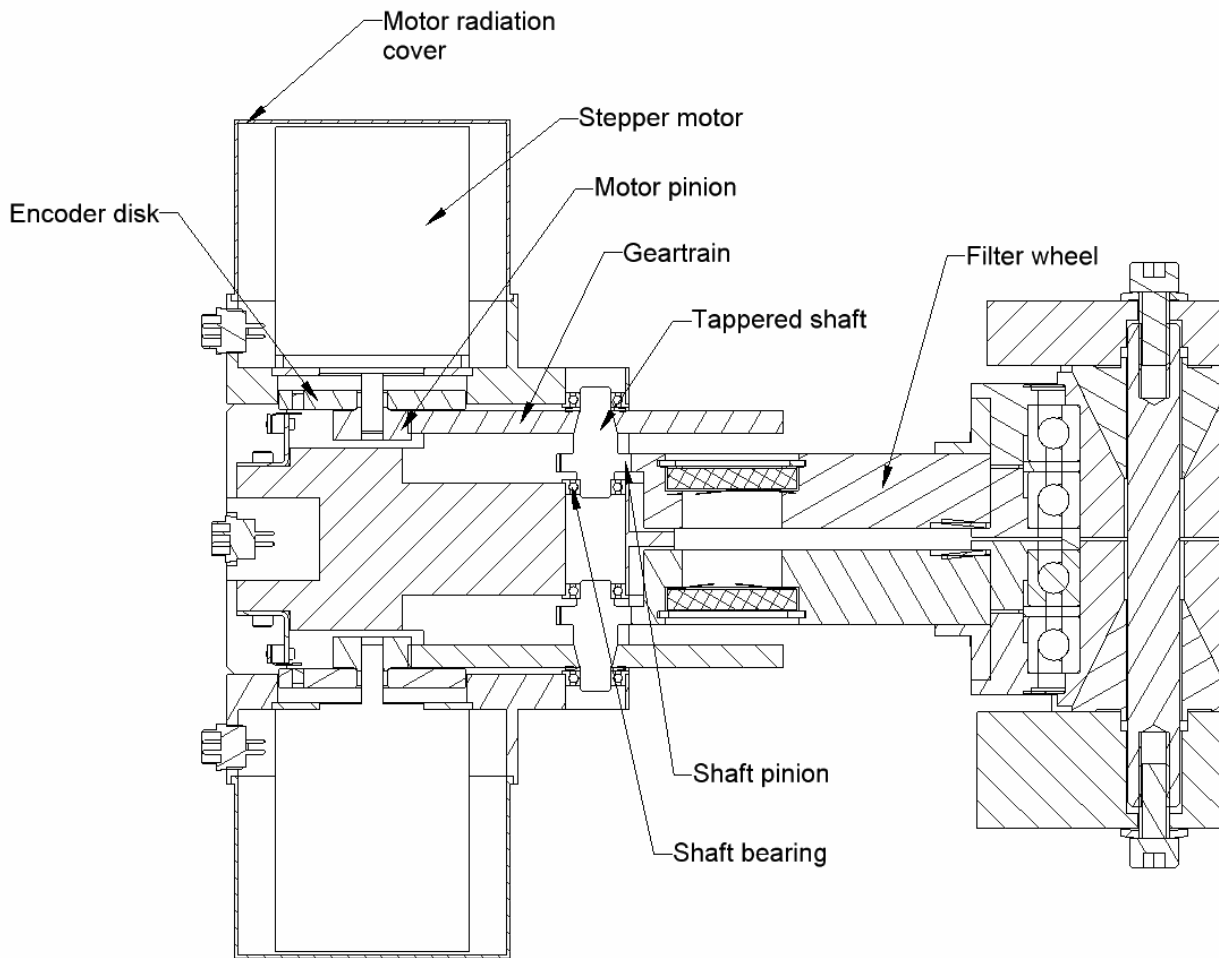


Fig. 7. Filter wheel transmission box – cross section.

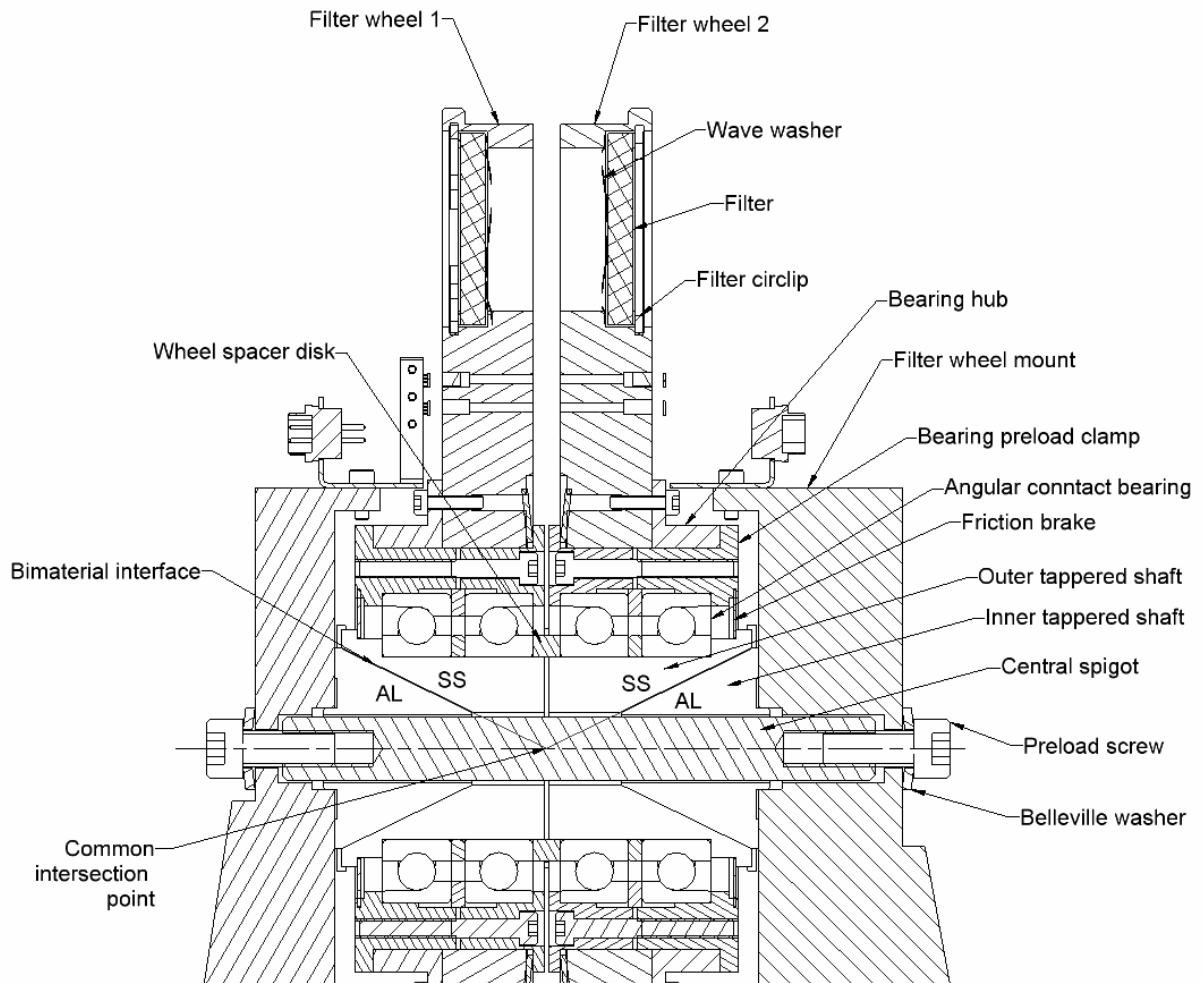


Fig. 8. Filter wheel bearing system – cross section.

Both wheels will rotate about the same fixed shafts on two pairs of precision angular contact bearings, as illustrated in Fig. 8. The bearing races are spaced by precision lapped spacer rings. The rings and bearings are then firmly clamped together to obtain a bearing preload, defined by the difference in the spacer ring thicknesses. The bearings are positioned on a steel outer tapered shaft. This shaft slides on the matching tapered surface of an aluminium inner shaft. Both shaft pairs, one pair in each wheel, are then clamped by the mount hubs through the central spigot and Belleville washer loaded pre-tension screws. The bearing preload is always constant, irrespective of the temperature, since all parts in this subassembly are made of stainless steel.

The essential feature of this assembly is its insensitivity to differential radial shrinkage on the interface between the steel and aluminium parts. This interface is the tapered surface so any differential shrinkage is transferred to a sliding motion of aluminium and steel parts along the common interface. The main feature of this athermal design is that the intersection of the two bimaterial interfaces is the central point of the assembly, the point that defines the vertical symmetry line. Consequently, this point always remains fixed during cooling, while all other elements contract towards it. This ensures that there can be no lateral asymmetrical movements of the elements that would otherwise cause misalignment between active filter positions.

The second bimaterial interface is between the bearing clamps and the filter wheels. Here, a sufficient radial clearance exists to accommodate differential contraction between the aluminium material of the wheels and the steel clamps. This clearance was defined to obtain a standard H7/h6 fit between these two elements when the system is cold.

4. CONCLUSION

This paper presents comprehensive methods to deal with issues related to differential contraction that exist at bimaterial interfaces in cryogenic opto-mechanical systems.

The method presented for lens mounting is shown to be mechanically simple and very effective in practice. It allows for a simple and safe alignment procedure with high precision and repeatability. More importantly, it can be applied to any lens system irrespective of the lens size or material.

The mechanism athermalization method used in designing the GSAOI filter wheel can be applied to any cryogenic mechanism. However, its implementation is more appropriate in mechanisms where relatively large bearing systems are used. Mechanical tolerances of the large elements are usually insufficient to obtain precise positioning of optical elements. This becomes even more emphasized when the design has to account for differential contraction between elements and to predict their movements during cooling.

REFERENCES

1. RSAA GSAOI Instrument Development Team, GSAOI Critical Design Review Documentation, Canberra, October 2003.
2. P. McGregor, J. Hart, D. Stevanovic, G. Bloxham, D. Jones, J. Van Harmelen, J. Griesbach, M. Dawson, P. Young and M. Jarnik, Gemini South Adaptive Optics Imager (GSAOI), Proc. SPIE V.2 5492-39, Glasgow UK, 2004.
3. J. S. Accetta (Editor), D. L. Shumaker (Editor), *The Infrared and Electro Optical Systems Handbook*, SPIE--The International Society for Optical Engineering, January 1993.
4. American Institute of Physics., Dwight E. Gray (Editor), *American Institute of Physics Handbook*, McGraw Hill Text; 3rd edition, June 1972.
5. *Journal of Chemical Physics*, 41(8), 2324.
6. *NBS Technical Note 993 (via GNIRS SDN 03.02.)*, US Gov Printing Office, Washington DC, 1979.
7. <http://ccd.ifa.hawaii.edu/gemini/niri/coldtest/3/>